d

Analysis Note:

Anti-flow of Kaon in Au+Au Collisions at $\sqrt{s_{NN}}$ = 3 - 3.9 GeV

Zuowen Liu, Li-ke Liu, Xing Wu, Guoping Wang

Abstract

In this note, we present the measurement of anti-flow of mesons in Au+Au collisions at $\sqrt{s_{NN}}$ = 3-3.9 GeV with the STAR experiment under its fixed target configuration at RHIC. Directed flow and elliptic flow of π, K^0_S and Λ are presented in different centrality, transverse momentum and rapidity intervals. π^+ and K^0_S show anti-flow at low p_T(p_T < 0.6 GeV/c) at 3-3.9 GeV. And the result have been compared with JAM model. Anti-flow of mesons at low p_T could be explained by shadowing effect from spectaor.

CONTENTS

1. ANALYSIS SETUP

This section describes the setup of analysis. The first part of this section introduces STAR Fixed Target(FXT) mode. Second one is dataset and event selection used in the analysis. Third, badrun rejection and centrality determination are discussed.

1.1. Introduction of FXT

There are two modes at RHIC-STAR, Fixed Target mode and Collider mode. FXT mode of STAR experiment covers center of mass energy($\sqrt{s_{\mathrm{NN}}}$) from 3 to 13.7 GeV, which extends the measurement to lower energy intervals. In this way, FXT mode could reach higher baryon density region(up to 750 MeV). To achieve this goal, One piece of gold foil would be fixed at the end of Time Projection Chamber(TPC) as target.[1] And the accelerated gold beam from west would collide with it. Fig. 1 shows the schematic plot for fixed target mode.

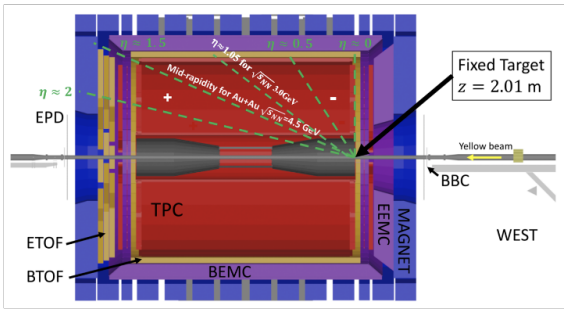

FIG. 1. The setup of Fixed Target mode at STAR.

The laboratory system should be transferred to the center of mass system, if one want to analysis physical observation conveniently. According to the Lorentz transformation, Rapidity(y) of the final state particle in the Center of Mass System(CMS) could be calculated as equation 1, where y_{lab} is rapidity of emitted particle in the laboratory frame, y_{beam} is rapidity of gold beam in the CMS. And we would discuss flow measurement based in the Center of Mass System.

$$y_{CMS} = y_{lab} - y_{beam} \tag{1}$$

TABLE I. Dataset and event cuts for $\sqrt{s_{\rm NN}} = 3, 3.2, 3.5, 3.9GeV$.

$\sqrt{s_{\rm NN}}$(GeV)	production tag	library tag	trigger ID	Vz(cm)	Vr (cm)
3.0	P19ic	SL20d	620052	[198, 202]	2
3.2	?	?	?	[198, 202]	2
3.5	P21id	SL21d	720000	[198, 202]	2
3.9	?	?	?	[198, 202]	2

1.2. Dataset and event selection

In this analysis, four energies($\sqrt{s_{\rm NN}} = 3, 3.2, 3.5, 3.9GeV$) from fixed target mode are involved. The events from minimum bias trigger are selected. And vertex cut in the X and Y direction applied to exclude the events from beam pipe, vertex cut along the Z direction to ensure that selection events are from collision on the gold foil. The detailed trigger and vertex cut are summarized in the TABLE. I

1.3. Badrun rejection and centrality determination

Data production at STAR is run-by-run type, and the data is tagged with different run number. Run-by-run QA is necessary to reject the bad runs, which may caused by the broken detector et al. This job was finished by STAR QA group, and the badrun list used in this analysis could be found at the summary page from QA group.

Moreover, the centrality determination work is vital in Heavy Ion Collision. Glauber Monte Carlo(MC) simulation[2] would describe the reference multiplicity distribution, which is corrected by pile-up rejection and luminosity correction. The number of participant particle(N_part) and the number of collision particles(N_coll) can be extracted by the formula 2 in MC model.

$$\frac{dN_{ch}}{d\eta} = n_{pp}\left[(1-x)\frac{N_{part}}{2} + xN_{coll}\right] \tag{2}$$

This work was finished by STAR Centrality group, a class(StRefMultCorr) is provided. One can call the class and get the refMult cut.

2. ANALYSIS METHOD

In this section, event plane reconstruction would be described firstly. Second part is identification for measured particles, including identified particles($pi+$ and $pi-$), and weak decay particles(K_0^S and Λ). Last one is efficiency correction, including TPC tracking efficiency, TOF matching efficiency and particle reconstruction efficiency.

2.1. Event plane reconstruction

Event plane method is one of common method in the anisotropic flow analysis, which could be used to estimate the reaction plane in the Heavy Ion Collision.[3] In this analysis, we used STAR detector Event Plane Detector(EPD), incorporating with Time Projection Chamber to reconstructe Event Plane(EP), where EPD is an upgrade detector in the STAR Beam Energy Scan phase II.[4] There are 12 supersectors on EPD. And 31 tiles on each supersector are connected via optical fiber bundles. The tile performance would be affected by its own quality and the signal intensity it received. So the correction for each tile is necessary, which would be introduced as follow.

Recentering and shifting method are two methods which we applied to correct the raw event plane distribution. EPD is divided to four ring groups to facilitate EP reconstruction. There are 16 rings/rows on EPD. It is divided equally to four groups, each group have four rings. Fig. 2 show groups at EPD, named as A, B, C and D. The best EP should be the one in the forward eta

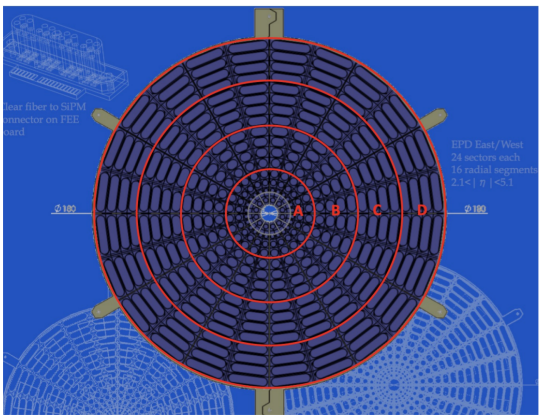

FIG. 2. The sketch of EPD groups.

range, where directed flow signal is greater than the one in middle eta range. Analysis note of one STAR published paper have approved it. We followed and chose EPD group A and B as target

event plane in our analysis. In this way, we can get the largest resolution applied to our analysis according to equation 3

$$R_n \propto v_n \sqrt{M} \tag{3}$$

2.1.1. *Recentering correction*

The recentering calibration is applied to the flow vector($\vec{Q}$), which could be decomposed into two components, as shown by equation 4, where w_i is EPD tile weight, using the calibrated value nMip(also known as ADC) based on the particle energy loss on each EPD tile, as shown by equation 5

$$\overrightarrow{\mathrm{Q}} = \begin{pmatrix} Q_y \\ Q_x \end{pmatrix} = \begin{pmatrix} \sum_i w_i \sin(\phi_i) \\ \sum_i w_i \cos(\phi_i) \end{pmatrix} \tag{4}$$

$$w(\text{ tile }) = \begin{cases} 0 & \text{if } nMIP < \text{threshold}(0.3) \\ \text{MAX} & \text{if nMIP } > \text{MAX}(2) \\ nMIP & \text{otherwise} \end{cases} \tag{5}$$

And the first order event plane angle could be obtained by equation 6, where ϕ_i is emitted particle angle with respect to the laboratory system, sums goes over all hits from one event.

$$\Psi_1 = \tan^{-1} \frac{\sum_i w_i \sin(\phi_i)}{\sum_i w_i \cos(\phi_i)} \tag{6}$$

The recentering method is applied to the flow vertex $\vec{Q}$, so it's event by event calibration, Which is expressed by equation 7. The angle brackets denote averaging over all events in the same centrality and run ID.

$$\vec{Q}_{rc} = \begin{pmatrix} \vec{Q}_y - \langle \vec{Q}_y \rangle \\ \vec{Q}_x - \langle \vec{Q}_x \rangle \end{pmatrix} \tag{7}$$

2.1.2. *Shifting correction*

The shifting calibration is a mathematical method to correct the EP distribution after recentering calibration, which is based on Fourier transformation. In this analysis, a 20th order equation 8 was implemented to the event plane distribution after recentering calibration.

$$\Psi_{1,\text{ shift}} = \sum_i^N \frac{2}{i} \left[-\langle \sin(i\Psi_{1,rc}) \rangle \cos(i\Psi_{1,rc}) + \langle \cos(i\Psi_{1,rc}) \rangle \sin(i\Psi_{1,rc}) \right] \tag{8}$$

The angle brackets in the equation denote averaging over all events in the same centrality and run ID. And the final EP angle after recentering and shifting calibration could be obtained by equation 9

$$\Psi_1 = \Psi_{1,rc} + \Psi_{1,shift} \tag{9}$$

Fig. 3 show event plane distribution at 3, 3.2, 3.5 and 3.9 GeV based on all EPD rings, where the black line show the raw distribution without any calibration, the blue line represents the EP after recentering calibration, and red line denote the event plane angle distribution after recentering and shifting calibration, which is "flat".

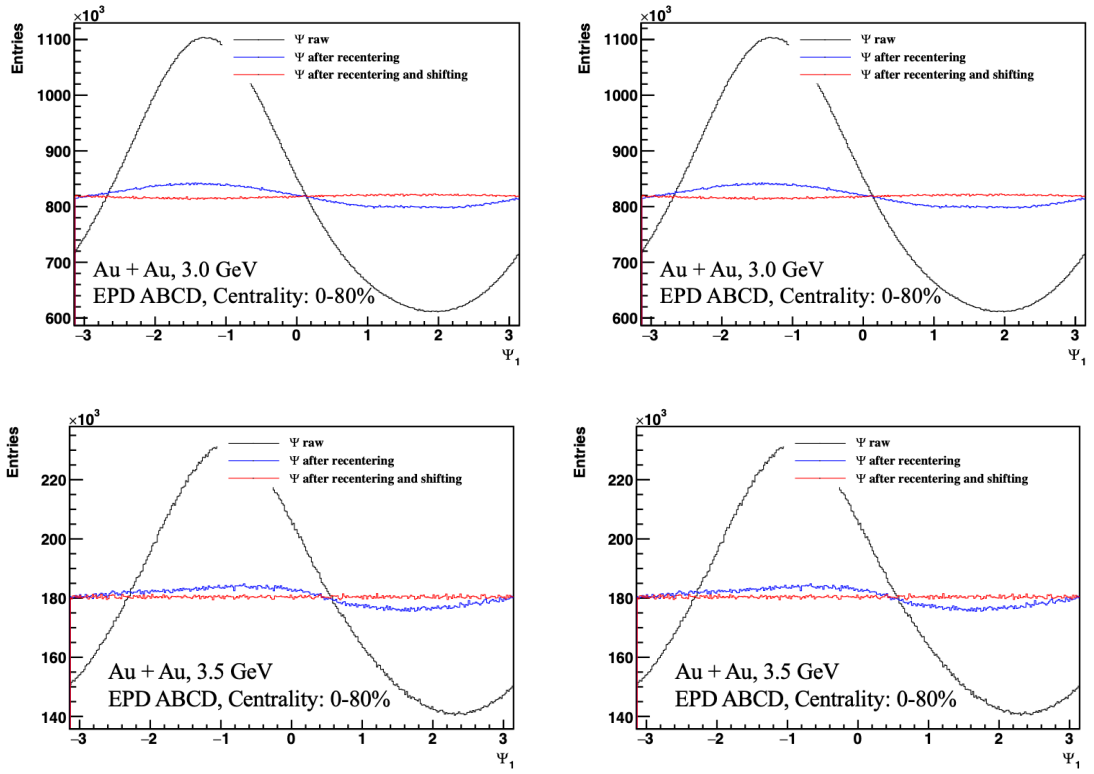

FIG. 3. The event plane distribution on EPD.

2.1.3. *Event plane resolution*

After recentering and shifting calibration, the event plane is ready for the flow calculation. While the finite multiplicity in the experiment would limit the estimation of the reaction plane angle. [5] So the event plane resolution would be brought to correct the oberverd flow coefficients,

which could be expressed as equation 10

$$R_n = \langle \cos\left[n\left(\Psi_n - \Psi_{\mathrm{r}}\right)\right]\rangle \tag{10}$$

Where Ψ_r is reaction plane angle, Ψ_n is the event plane angle. The angle brackets denote averaging over many events.

In the fixed target mode, one would not be able to get sub-events are equal, since the collision happens at the end of TPC. The resolution in different window are not equal, one need at least three windows to determine the event plane resolution in each of them. [6] It could be expressed as

$$\langle \cos\left(n\left(\Psi_m^a - \Psi_r\right)\right)\rangle = \sqrt{\frac{\langle \cos\left(n\left(\Psi_m^a - \Psi_m^b\right)\right)\rangle \langle \cos\left(n\left(\Psi_m^a - \Psi_m^c\right)\right)\rangle}{\langle \cos\left(n\left(\Psi_m^b - \Psi_m^c\right)\right)\rangle}} \tag{11}$$

Where Ψ_m^a is the target event plane angle, Ψ_m^b and Ψ_m^c are the reference event plane angle.

In this analysis, we foucus on directed flow(v_1) and elliptic flow(v_2) measurement, they are both bashed on first order event plane. so we substitue $m = 1$ to the equation 11. According to the STAR published 3 GeV paper [7], One can get the largest resolution if chosen the forward eta window(EPD group A and B). We follow the method and take EPD group A and B as our target event plane. Other windows from EPD and TPC would be chosen as reference windows. They are divided as shown by Fig. 4 This figure is specical for 3.0 GeV. We note here eta could reach 2.4 for 3.2, 3.5 and 3.9 GeV data, since inner TPC was upgarded at these three energies, and eta gap in the TPC is $[-1.15, -1.25]$.

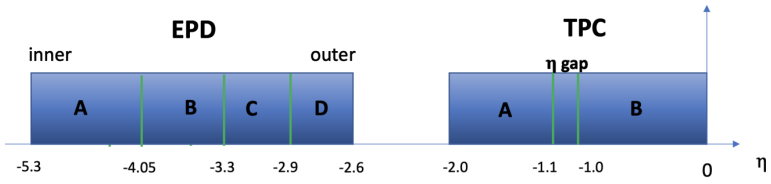

FIG. 4. The sketh of EPD and TPC groups.

2.2. Particle identification

2.3. Efficiency correction

Appendix A: appendix

[1] M. S. Abdallah *et al.* (STAR Collaboration), Phys. Rev. C **103**, 034908 (2021).

[2] D. Kharzeev and M. Nardi, Physics Letters B **507**, 121 (2001).

[3] A. Bilandzic, R. Snellings, and S. Voloshin, Phys. Rev. C **83**, 044913 (2011).

[4] J. Adams *et al.*, Nuclear Instruments and Methods in Physics Research Section A: Accelerators, Spectrometers, Detectors and Associated Equipment **968**, 163970 (2020).

[5] S. A. Voloshin, A. M. Poskanzer, and R. Snellings, "Collective phenomena in non-central nuclear collisions," (2008), arXiv:0809.2949 [nucl-ex].

[6] A. M. Poskanzer and S. A. Voloshin, "Methods for analyzing anisotropic flow in relativistic nuclear collisions," (1998), arXiv:nucl-ex/9805001 [nucl-ex].

[7] M. Abdallah *et al.* (STAR Collaboration), Physics Letters B **827**, 137003 (2022).